Available online at www.sciencedirect.com
ScienceDirect
Geochimica et Cosmochimica Acta 71 (2007) 1341–1354
Geochimica
www.elsevier.com/locate/gca

Mass independently fractionated sulfur components in chondrites

Vinai K. Rai *, Mark H. Thiemens

Department of Chemistry and Biochemistry, University of California San Diego, La Jolla, 92093-0356 CA, USA

Received 27 April 2006; accepted in revised form 27 November 2006

Abstract

We report high precision sulfur isotopic data obtained by sequential extraction from various physically separated phases (bulk, matrix, and chondrules) from chondrites. A significant excess of ^{33}S (up to $\Delta^{33}S$ of 0.112‰ for Dhajala Chondrule) has been observed and is most likely carried by chondrule rims, though chondrule interiors cannot be ruled out as a carrier. Stellar nucleosynthesis and spallation are ruled out as a cause for this anomaly. Photochemical irradiation of sulfur gaseous species in the early solar nebula has, most likely, produced this anomaly. Observations of mass independent sulfur of photochemical origin suggest that chondrules and their rims must have formed in an optically thin nebular region. This also suggests that the chondrules were formed near the protoSun when it was active in ultraviolet light emission.

1. Introduction

Sulfur is one of the more important elements in geo and cosmochemistry. In the reduced environments of the early solar nebula (where Enstatite chondrites or Aubrites were formed) sulfur is somewhat analogous to oxygen in that it condenses to refractory solids from a nebular gas with a ratio C/O >1, but otherwise solar in composition. Sulfur condensation initiates in a reducing environments at high temperatures, with CaS, MgS, AlN, and SiC appearing in the condensation sequence concomitantly with corresponding oxides (Larimer and Bartholomay, 1979). Reduced environments of the early solar nebula could be produced locally either from diffusive removal of water (Pasek et al., 2005) or by evaporation of carbon rich grains (Larimer and Bartholomay, 1979). Sulfur is particularly interesting as it possesses four stable isotopes which may be utilized to quantify various sulfur components present in meteorites. Sulfur is the only multi-isotopic element other than oxygen, where mass independent fractionation (MIF) has been observed both in nature as well as in laboratory experiments. As such, it is a sensitive probe of chemical reactions. Unlike oxygen, where more than one process can produce mass independent isotopic compositions (Thiemens and Heidenreich, 1983; Thiemens, 1999; Gao and Marcus, 2001; Miller et al., 2002), mass independent sulfur is in most cases produced by photochemical reactions (Farquhar et al., 2000c, 2001). Precise measurements of sulfur isotopes in primitive meteorites may thus uniquely serve as a potential isotopic marker of photochemical processes in the early solar nebula and enhance our understanding of the origin of isotopic anomalies for other elements, particularly oxygen where it is likely that photochemistry is important.

Mass independent sulfur has been observed in a variety of natural samples such as present day sulfate aerosols in the Earth's atmosphere (Romero and Thiemens, 2003), Archean sediments (Farquhar et al., 2000a), sulfur inclusions in kimberlitic diamonds (Farquhar et al., 2002), Martian regolith (Farquhar et al., 2000c), achondritic meteorites (Farquhar et al., 2000b; Rai et al., 2005) and sulfonic acid extracts from the Murchison (CM) meteorite (Cooper et al., 1997). It has been demonstrated that the sulfur products obtained during UV photolysis of sulfur dioxide fractionate mass independently. Mass independent sulfur has also been observed in the product of H_2S

* Corresponding author. Fax: +1 858 534 7042.
E-mail address: rai@chem.ucsd.edu (V.K. Rai).

0016-7037/$ - see front matter © 2006 Elsevier Inc. All rights reserved.
doi:10.1016/j.gca.2006.11.033

photolysis (Farquhar et al., 2000c). A recent review of mass independent isotopic components is given by Thiemens (2006).

Chondrites are the most primitive group of meteorites, composed predominantly of millimeter sized chondrules cemented together by fine grained matrices. Chondrules are rounded objects, composed mainly of ferromagnesian silicates with Fe–Ni metal and minor sulfides (Hewins, 1997). They are one of the earliest formed solids in the solar system (Taylor et al., 1983; Grossman, 1988), along with CAIs (formed within a few million years of one another). These are igneous objects that exhibit evidence of having undergone transient episodes of heating followed by rapid cooling before incorporation into chondrites. Although the mineralogy, bulk chemistry, and textural properties of typical chondrules provide constraints on their formation, the exact mechanism of chondrule formation is still not well understood. The bulk chemical composition of chondrules, in general, is very similar to that of CI chondrites except for volatile lithophile elements which are depleted in Chondrules (Hewins, 1997). Chondrules in most cases are surrounded by a fine grained rim, which is shown to be relatively rich in volatiles as compared to bulk chondrules. There are several types of chondrules observed in chondrites and all varieties of chondrules are mostly present in each chondrite class, however the proportions vary significantly (Sears, 2004).

Several models have been proposed for the origin of chondrites and chondrules (Boss, 1996). Among them nebular shock wave models (Hood and Horanyi, 1993; Connolly and Love, 1998; Ciesla and Hood, 2002; Desch and Connolly, 2002) and x-wind models (Shu et al., 1996) have received considerable attention recently as potential chondrule forming processes. In the x-wind model, both chondrules and CAIs and their rims originated at a distance of about 0.6 AU (13 times the radius of the Sun) and were ejected to planetary distances by the solar x-wind, where they aggregated with the ambient dust to form larger chondritic bodies whereas in nebular shock wave models, chondrules were formed near the mid plane of the disk with shock wave processing of ambient grains or dust. In addition to these nebular models, there are other groups which suggest asteroidal collision as the origin of chondrules (Symes et al., 1998; Ruzicka et al., 2000).

Recently Rai et al. (2005) reported the presence of MIF sulfur in differentiated meteorites. It is striking that despite several detailed studies of sulfur in primitive chondrites, anomalous sulfur has not been observed (Hulston and Thode, 1965; Gao and Thiemens, 1993a,b) except for a few isolated instances (Rees and Thode, 1977). Later attempts to replicate this anomaly were not successful (Rees and Thode, 1977; Gao and Thiemens, 1993a,b) indicating that the observed anomaly is either an artifact or that the carrier of anomalous sulfur is heterogeneously distributed. Chondrites, being the most primitive meteorite class, are the most likely to possess an anomalous isotopic composition for any element. However, after extensive measurements, sulfur has been demonstrated to be strictly normal. The reason may be twofold (1) MIF sulfur was not present in the solar nebula and the observation of such sulfur in differentiated meteorites is not of nebular origin and is produced by an anomalous, undefined parent body processes or, (2) MIF sulfur exists in chondrites but is not readily observed because of an overwhelming presence of larger amounts of sulfur of normal isotopic composition. In order to search for anomalous sulfur, we have initiated a study of sulfur isotopes in various phases of chondrites e.g., fine grained matrix, chondrule interiors and rims to shed new light on the origin of chondrules and chondrites. In this study, we investigate the sulfur isotopic composition of these physically separated components by a sequential leaching method.

It is now established that sulfur undergoes mass independent fractionation during UV photolysis of gaseous sulfur species present in the early solar nebula and Earth (Colman et al., 1996; Farquhar et al., 2000c, 2001). A precise study of sulfur components also has potential bearing on the origin of chondrites and provides a test for various models of chondrite formation, particularly the x-wind model (Shu et al., 1996). In the x-wind model for chondrule formation, chondrule precursors from an optically opaque disk were processed through the x-region and subsequently launched back to the disk by an x-wind (Shu et al., 1996). If the fine grained rim of chondrules were condensed on nucleation centers of the protochondrules while the wind expands and cools (Shu et al., 1996) when lifted out of the disk by the x-wind, they would have been exposed to intense UV light from the protoSun. It is therefore possible that sulfur in both bulk chondrules and their rims might have experienced strong solar UV light from a protoSun and a study of sulfur isotopes in matrix, chondrule interiors and rims might provide both spatial and temporal information regarding chondrule formation.

2. Sample preparation and experimental procedure

2.1. Sample preparation

In Table 1, chondrites analyzed in this study are listed along with their metamorphic grade and weathering

Table 1
Source and details of the chondrites selected for this study

Met. (Class, WC)	Source	Bulk	Matrix	Chondrule
Allende (CV3)	FMNH[a]			√
Dhajala-1 (H3.8)		√		√
Dhajala-2 (H3.8)	JNG[b]		√	√
EET99404 (H4, B)	JSC[c]		√	√
ALH85033 (L4, A)	JSC		√	√
Hvittis (EL6)	FMNH	√		

[a] Field Museum of Natural History, Chicago.
[b] Sample obtained form J.N. Goswami, PRL, India.
[c] Johnson Space Center, NASA; WC, weathering category.

category (for Antarctic Finds). Bulk samples of chondrites were washed with Millipore water before chemical extraction of sulfur. Chondrules from individual chondrites were desegregated using freeze–thaw technique and were hand picked under a binocular microscope. Subsequently these chondrules were washed with Millipore water several times before chemical extraction of sulfur was done. Nearly 500 mg of chondrule fractions composed of all types present (separation based on their size and type was not attempted) was used for sulfur extraction. Fine grained matrix is the material that remains floating after shaking or perturbation during washing with Millipore water during freeze–thaw desegregation. These materials ultimately settle to the flask bottom if left undisturbed and are recovered after evaporating the water in a drying oven. Sulfur in most cases was extracted in several steps and the number of steps was evaluated based upon the size of the samples and sulfur concentration.

2.2. Sulfur extraction and fluorination

The chemical extraction procedure of sulfur employed here is essentially the same as described by Hulston and Thode (1965). Approximately a few hundred milligrams of sample was powdered with a steel mortar and pestle and transferred to a 50 ml boiling flask. Acid volatile sulfur (sulfide phases) evolved as H_2S after reaction with 6N HCl bubbled through cadmium acetate (0.2 M) with high purity nitrogen as the carrier gas through water trap using an apparatus described by Forrest and Newman (1977). H_2S quickly reacted with cadmium acetate to form cadmium sulfide, which precipitated as silver sulfide by adding (0.2 M) silver nitrate. Once the sufficient cadmium sulfide had been accumulated as visualized by yellow colored cadmium sulfide, old trap of cadmium acetate was replaced by fresh ones. Initially these reactions were done at room temperature. However, when the last one did not yield sufficient cadmium sulfide for isotopic analysis, the reaction temperature was increased to 100 °C. Silver sulfide was subsequently filtered, dried, and weighed to calculate the percentage weight of sulfur as sulfide. Nearly 2 mg of silver sulfide was transferred to an aluminum boat and loaded into a nickel tube for fluorination overnight at 580 °C. Product SF_6 was separated from other byproducts and unreacted BrF_5 with multiple stage ethanol slush at −119 °C and was further purified by gas chromatography using a 1/8-in diameter, 12-ft long column packed with Porapak-Q. High purity helium was used as the carrier gas. Ethanol slush at −119 °C was also applied to the sample tube before collecting SF_6 on the mass spectrometer cold finger for isotopic analysis. In all the samples, the remaining HCl after sulfide extraction, was evaporated to dryness. Subsequently, sulfate extraction was performed using a reduction solution following the procedure of Gao and Thiemens (1993a). Except for Dhajala-1 Chondrule (which is also very small), none of the samples yielded measurable amount of sulfate.

The isotopic composition was measured as SF_5^+ ion (mass to charge ratios of 127, 128, 129, and 131) on a Finnigan MAT 252 triple collector isotope ratio mass spectrometer at UCSD. Isotopic compositions are reported in conventional delta notation defined as:

$$\delta^i\mathrm{S}(‰) = \left[\left({}^iR_{\mathrm{sample}}/{}^iR_{\mathrm{standard}}\right) - 1\right] \times 1000 \quad (1)$$

where ${}^i\mathrm{R} = {}^i\mathrm{S}/{}^{32}\mathrm{S}$ and i is mass of the individual isotopes, which are 33, 34, and 36 in the case of sulfur. All sulfur isotope data are reported with respect to Cañon Diablo troilite. The Δ^{33}S and Δ^{36}S values are calculated using the following equation:

$$\Delta^j\mathrm{S}(‰) = \delta^j\mathrm{S} - 1000\left[(1 + \delta^{34}\mathrm{S}/1000)^{\lambda} - 1\right], \quad (2)$$

where j is mass 33 and 36, and λ are obtained empirically; 0.5114 ± 0.0014 and 1.895 ± 0.010 for Δ^{33}S and Δ^{36}S, respectively (see Section 3 for further details).

2.3. Standard analyses and precision

We have performed a large number of standard analyses on commercially available silver sulfide and troilite from Cañon Diablo to determine the precision and reproducibility of our analyses. The typical errors (1σ) in δ^{33}S, δ^{34}S, and δ^{36}S mass spectrometer measurements are ±0.010‰, 0.010‰, and 0.100‰, respectively, though the individual errors of each measurement (which depends on sample size and several other parameters) are tabulated along with δ values in Table A1. The typical errors of individual Δ^{33}S and Δ^{36}S are ±0.010‰ and 0.100‰, respectively. During the course of this study, we have analyzed 11 CDT standards which yielded a mean value of $\Delta^{33}\mathrm{S} = 0.001 \pm 0.007$‰ with a standard error value of 0.002 (11 measurements), whereas the mean value of δ^{34}S is -0.135 ± 0.126 (standard error of 0.038) (Rai et al., 2005). Additional information about the reproducibility and IAEA standard analyses from the lab at UCSD may be found in Gao and Thiemens (1993a). Since the variation of sulfur isotope composition during chemical processing and measurements are mass dependent, the relatively lower overall precision of δ values do not really affect the precision of Δ^{33}S and Δ^{36}S which are much smaller.

To ensure that the variations of Δ are not an artifact of the stepwise extraction procedure, a homogeneous sulfur reservoir was prepared by oxidizing commercially available silver sulfide with fuming nitric acid and subsequently determining the sulfur isotopic composition using stepwise extraction with a standard reduction solution (Forrest and Newman, 1977; Gao and Thiemens, 1993a). The data are displayed in Fig. 1. Despite experiencing large isotopic fractionations during stepwise extraction, the Δ^{33}S values of the samples were indistinguishable within the experimental uncertainty, indicating that the stepwise extraction procedure used for sulfur isotopes strictly obeys the mass fractionation law and any deviation observed from mass dependent fractionation in natural samples is real.

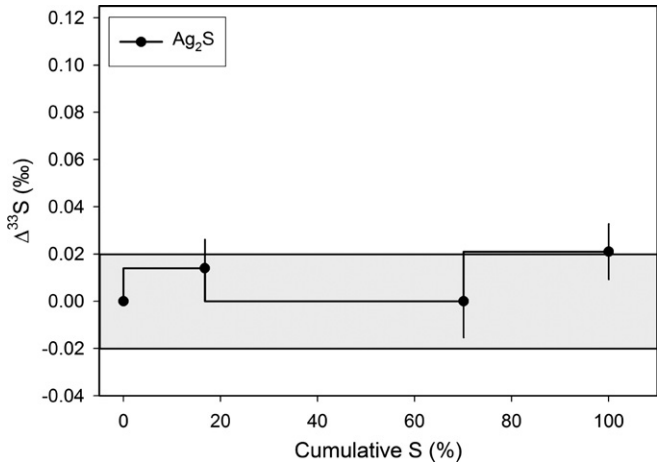

Fig. 1. Plot of $\Delta^{33}S$ values versus cumulative percent of sulfur release in each steps from commercially available silver sulfide which shows that $\Delta^{33}S$ values obtained in various steps are same within experimental uncertainty. $\Delta^{33}S$ values are calculated using an exponent of 0.512.

3. Results

3.1. Determination of exponent λ for mass fractionation experiment in laboratory

Most chemical and biological processes in nature fractionate sulfur isotopes mass dependently i.e., the variation in $\delta^{33}S$ is always one half of $\delta^{34}S$ and variation in $\delta^{36}S$ is nearly twice of $\delta^{34}S$. Theoretical formulations for equilibrium isotopic fractionations have been developed and are discussed in Urey (1947) and Bigeleisen and Mayer (1947); and later calculations were further extended to the sulfur compounds by Tudge and Thode (1950). Hulston and Thode (1965) showed that for a smaller range of fractionation, sulfur isotopes obey the following equations:

$$\delta^{33}S = 0.515\delta^{34}S \tag{3}$$

and

$$\delta^{36}S = 1.89\delta^{34}S. \tag{4}$$

These relations can be extended further to a larger range of fractionations (Hulston and Thode, 1965) provided δ values are redefined in logarithmic form i.e.,

$$\delta'^{i}S = 1000\ln\left[\left({}^{i}S/{}^{32}S\right)_{sample}/\left({}^{i}S/{}^{32}S\right)_{std}\right]. \tag{5}$$

Substituting this expression into equation (3) and rearranging yields:

$$\ln\left[\left({}^{33}S/{}^{32}S\right)_{sample}/\left({}^{33}S/{}^{32}S\right)_{std}\right] = 0.515\ln\left[\left({}^{34}S/{}^{32}S\right)_{sample}/\left({}^{34}S/{}^{32}S\right)_{std}\right]$$

or

$$\left[\left({}^{33}S/{}^{32}S\right)_{sample}/\left({}^{33}S/{}^{32}S\right)_{std}\right] = \left[\left({}^{34}S/{}^{32}S\right)_{sample}/\left({}^{34}S/{}^{32}S\right)_{std}\right]^{0.515}. \tag{6}$$

After converting ratios to conventional δ notations, we obtain,

$$\left[\left({}^{33}S/{}^{32}S\right)_{sample}/\left({}^{33}S/{}^{32}S\right)_{std}\right] - 1 + 1 = \left[\left({}^{34}S/{}^{32}S\right)_{sample}/\left({}^{34}S/{}^{32}S\right)_{std} - 1 + 1\right]^{0.515} 1 + \delta^{33}S/1000 = \left[1 + \delta^{34}S/1000\right]^{0.515} \text{ or,}$$

$$\delta^{33}S = 1000\left[\left(1 + \delta^{34}S/1000\right)^{0.515} - 1\right], \tag{7}$$

in the same way,

$$\delta^{36}S = 1000\left[\left(1 + \delta^{34}S/1000\right)^{1.89} - 1\right]. \tag{8}$$

In any natural fractionation process, sulfur isotopes obey Eqs. (7) and (8). The exponential factors 0.515 and 1.89 were obtained theoretically after a number of approximations or assumptions and were never verified experimentally. It is vital to determine these values precisely in the laboratory if one is dealing with very small deviations (Δs) from the mass dependent curve defined by Eqs. (7) and (8). Since meteorites exhibit a very narrow range of isotopic fractionations (Gao and Thiemens, 1991, 1993a,b; Rai et al., 2005), the deviations from the mass fractionation curve are measured as Δ values and are expected to be very small. We performed laboratory fractionation experiments to obtain the precise exponential factors using commercially available silver sulfide. Prior to step wise extraction of sulfur (as cadmium sulfide), silver sulfide is oxidized to barium sulfate by reaction with fuming nitric acid followed by barium chloride in order to ensure an isotopically homogeneous sulfur reservoir. Subsequently sulfur was extracted in three steps which exhibit a relatively larger range of fractionation which is ideal for precisely obtaining the exponential factors. Three more aliquots of the same silver sulfide were also analyzed where all sulfur was extracted in a single step with reaction with 6N HCl. The δ values obtained are plotted as 1000 ln $[1 + \delta^{33}S/1000]$ and 1000 ln $[1 + \delta^{36}S/1000]$ on the y-axis against 1000 ln $[1 + \delta^{34}S/1000]$ on the x-axis (Fig. 2) and the slope of these two sets of lines provide required exponential values (see Eqs. (6)) (Miller, 2002). It can be seen clearly that all the data regressed along well defined lines with corresponding slope values of 0.5114 ± 0.0014 ($R^2 = 0.999971$) and 1.895 ± 0.010 ($R^2 = 0.999989$). The nonzero intercept value of $\delta^{36}S$ is due to CDT normalization of Ag_2S which has non zero value of $\Delta^{36}S$. We use these values to calculate $\Delta^{33}S$ and $\Delta^{36}S$ in Table A1 rather than 0.515 and 1.91 used previously (Farquhar et al., 2002). Use of these values is further justified by the observation of a similar slope values for the regression lines on three isotope plot of sulfur isotope data from chondrites

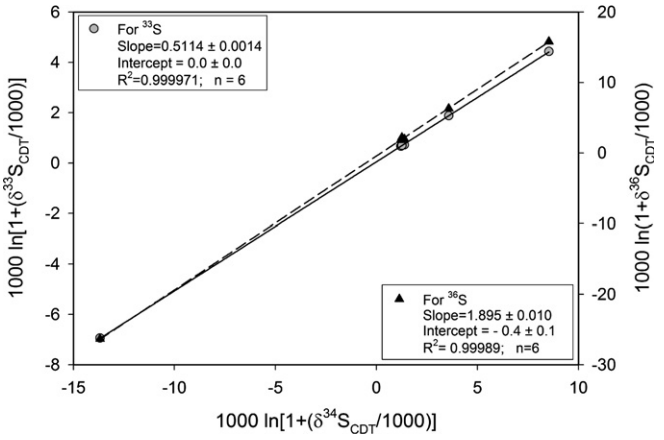

Fig. 2. The function 1000 $\ln[1+(\delta^{34}S/1000)]$ are plotted against 1000 $\ln[1+(\delta^{33}S/1000)]$ and 1000 $\ln[1+(\delta^{36}S/1000)]$ to obtain the values of exponents (in Eq. 3) during chemical fractionation experiment in laboratory on commercial silver sulfide by step extraction. It can be seen clearly that the exponents obtained are quite different than those used in literature.

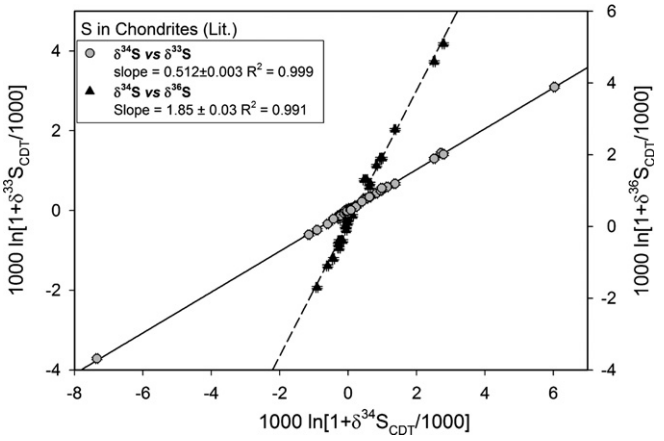

Fig. 3. The function 1000 $\ln[1+(\delta^{34}S/1000)]$ are plotted against 1000 $\ln[1+(\delta^{33}S/1000)]$ and 1000 $\ln[1+(\delta^{36}S/1000)]$ for chondrites from literature. It can be seen that the slope values are quite similar to those obtained in laboratory fractionation experiment (Fig. 2).

obtained from the literature (see Fig. 3). When $\delta^{33}S$, $\delta^{34}S$, and $\delta^{36}S$ from all the chondrite data are plotted on a similar three isotope plot, the regression lines have the slope values 0.5122 ± 0.0026 and 1.850 ± 0.034.

3.2. Sulfur in bulk or matrix samples

3.2.1. Total sulfur composition

Sulfur is extracted stepwise from two bulk samples of Dhajala and Hvittis and fine grained matrix from Dhajala, EET99404, ALH85033, and chondrules from Allende, Dhajala, EET99404, ALH85033. The isotopic composition of each individual step are reported in Table A1 and summarized in Table 2. Hvittis has previously been analyzed for sulfur isotopes (Gao and Thiemens, 1993b) and has a $\delta^{34}S$ value of $-0.16‰$ as compared to $-0.043‰$ observed in this study. $\Delta^{33}S$ and $\Delta^{36}S$ values obtained for Hvittis are $-0.029‰$ and $0.037‰$, respectively, and are similar within experimental uncertainty to that obtained from the literature ($-0.02‰$ and $-0.10‰$). All three ordinary chondrites are measured first time for sulfur isotopes. Bulk samples of Dhajala contain nearly 2 wt% of sulfur with a mean $\delta^{34}S$ value of $-0.055‰$, which falls within the range observed in the literature for ordinary chondrites (Table 2). The mean values of $\Delta^{33}S$ and $\Delta^{36}S$ are 0.014% and 0.138‰, respectively, and are also indistinguishable from the corresponding mean values for ordinary chondrites (Table 2).

3.2.2. Stepwise release

The data of Dhajala-1 bulk and Dhajala-2 fine grained matrix samples were extracted in four and three steps, respectively (Table A1), and possess 2.0 and 2.3 wt% S, respectively. Dhajala-1 bulk showed $\delta^{34}S$ values from $-0.937‰$ in the first step to $0.869‰$ in the third step whereas the corresponding values for matrix sample of Dhajala-2 are -0.146 (first step) and 0.353 (second step). In Fig. 4a, the $\Delta^{33}S$ of sulfur released are plotted against the cumulative percentage of sulfur extracted. It can be seen clearly that in both the samples, $\Delta^{33}S$ increases with increasing extraction step and the corresponding highest $\Delta^{33}S$ values are $0.071‰$ and $0.041‰$ which are clearly resolved over analytical uncertainty. It is interesting to note that the weighted mean of both samples are the same within the analytical uncertainty and indistinguishable from zero.

In EET99404 matrix sample, sulfur is extracted in four steps and has 1.4 wt% of sulfur as sulfide phase. Its $\delta^{34}S$ values ranges from $-0.215‰$ (first step) to $0.377‰$ (second step) with abundance weighted mean value of all the steps $-0.133 \pm 0.005‰$ (Fig. 4c). The $\Delta^{33}S$ of all the steps are remarkably constant indicating that the sulfur in all the steps was derived from one single component.

Sulfur in ALH85033 matrix was extracted in two steps and has a total 1.8 wt% of sulfur as sulfide. It possesses $\delta^{34}S$ values of $-0.214‰$ and $1.007‰$ in the first and last step, respectively (Table 2 and Fig. 4d). $\Delta^{33}S$ values for both the steps are $0.010‰$ and $0.031‰$, respectively.

Sulfur in Hvittis was extracted in six steps with $\delta^{34}S$ values range from $-1.467‰$ in the last step to $2.265‰$ in third step (Table 2). It has 3.0 wt% sulfur with weighted mean of $\delta^{34}S$ from all the steps of $-0.043 \pm 0.005‰$. $\Delta^{33}S$ of each step are plotted against cumulative percentage S release in Fig. 4b. It can be seen clearly that $\Delta^{33}S$ starts at $-0.031‰$ and $-0.037‰$ in the first and second steps and increase up to $0.014‰$ i.e., a total range of variation in $\Delta^{33}S$ of $0.051‰$, which is greater than analytical uncertainty. The weighted mean of $\Delta^{33}S$ is $-0.029‰$, which is lower than the average of enstatite chondrites from the literature $-0.007 \pm 0.014‰$ (mean of eight measurements) (Gao and Thiemens, 1993b).

3.2.3. Sulfur in chondrules

Dhajala. Sulfur from Dhajala (H3.8) chondrules was extracted twice, in three and six steps, respectively, for

Table 2
Summary of sulfur isotope composition extracted by sequential leaching from various chondrites and their components with respect to CDT along with data from literature

Sample name	S% (wt.)	Range $\delta^{34}S$ (‰)	Mean $\delta^{34}S$	Range $\Delta^{33}S$ (‰)	Mean $\Delta^{33}S$	Range $\Delta^{36}S$ (‰)	Mean $\Delta^{36}S$
Allende chondrule	0.89	−0.965 to 0.692	0.084	0.009 to 0.023	0.018	−0.251 to 0.190	−0.039
Allende broken chondrules	1.78						
Dhajala-1 bulk	1.98	−0.931 to 0.869	−0.055	0.071 to 0.002	0.014	−0.102 to 0.190	0.138
Dhajala-1 chondrule	0.76	−1.067 to 0.995	−0.068	−0.001 to 0.113	0.025	−0.185 to 0.072	−0.129
Dhajala-1chondrule (sulfate)[c]	0.004		2.411		0.148		−2.140
Dhajala-1 chondrule + matrix	1.70	−0.308 to 0.855	0.089	−0.001 to 0032	0.010	−0.041 to 0.057	−0.008
Dhajala-2 chondrule	0.90	−0.895 to 1.226	−0.027	−0.004 to 0.088	0.016	−0.215 to −0.028	−0.155
Dhajala-2 matrix	2.29	−0.146 to 0.352	0.178	0.004 to 0041	0.009	0.048 to 0.178	0.098
EET99404 chondrule	1.24	−0.155 to 1.301	0.089	0.001 to 0032	0.003	−0.215 to 0.281	0.189
EET99404 matrix	1.40	−0.215 to 0.377	−0.133	0.002 to 0.010	0.008	−0.126 to 0.033	−0.097
ALH85033 chondrule	0.92	−0.654 to 1.218	0.006	−0.026 to 0.021	−0.017	−0.140 to −0.005	−0.048
ALH85033 matrix	1.84	−0.214 to 1.007	0.085	0.010 to 0.031	0.015	−0.126 to −0.088	−0.117
Hvittis bulk	2.98	−1.467 to 2.265	−0.043	−0.037 to 0.014	−0.029	−0.114 to 0.220	0.037
From literature[b]							
Carbonaceous chondrites		−7.32 to 6.05			0.012 ± 0.027 (15)[a]		−0.027 ± 0.148(8)
Ordinary chondrites		−0.12 to 0.59			0.005 ± 0.028 (14)		0.278 ± 0.131 (4)
Enstatite chondrite		−0.39 to −0.16			−0.007 ± 0.014 (8)		−0.049 ± 0.067(5)
Mean achondrite		−0.577 to 1.710			0.040 ± 0.006		−0.013 ± 056
Allende chondrule (Size sorted)		−0.07 to 0.32		0.00 to 0.05		−0.1 to 0.3	

[a] Numbers in parentheses are number of measurements.
[b] Carbonaceous chondrite and Allende chondrule data are from Gao and Thiemens (1993a) and ordinary and enstatite chondrite data are from Gao and Thiemens (1993b); Achonrdite data from Rai et al. (2005) and Farquhar et al., 2000b.
[c] Yield of sulfur is very small and may be contaminated.

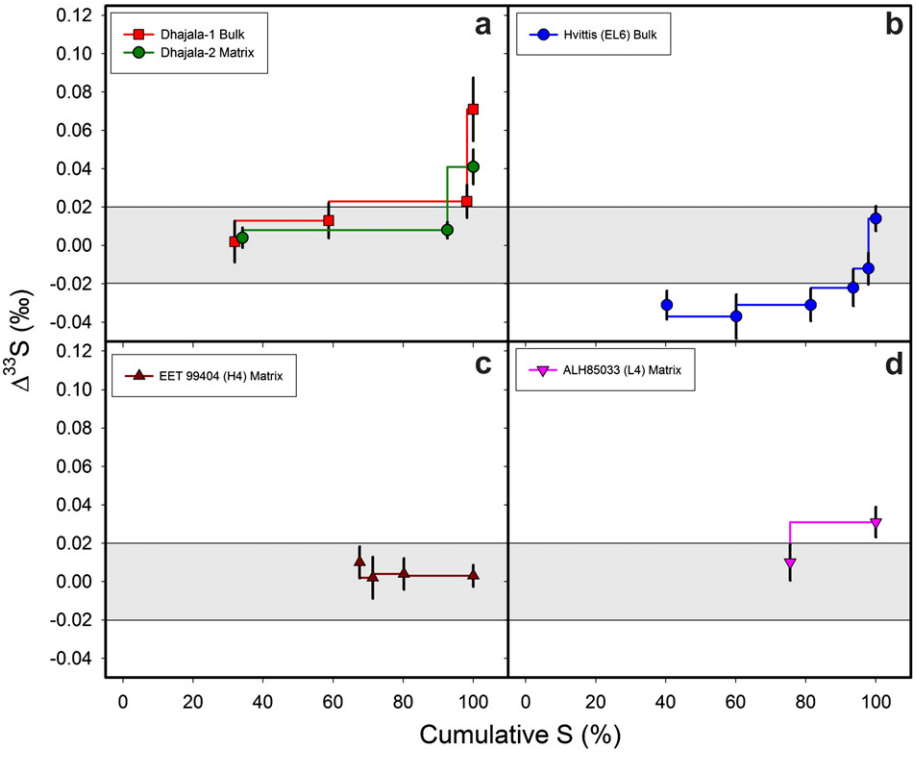

Fig. 4. $\Delta^{33}S$ of various steps are plotted against cumulative sulfur release for bulk and matrix samples of chondrites. The shaded rectangle represents 2σ error envelope. $\Delta^{33}S$ values are calculated using 0.512 as the exponent.

Dhajala-1 and Dhajala-2 (see Tables 1 and A1). They have a total of 0.8 and 0.9 wt% sulfur with weighted averages for $\delta^{34}S$ of $-0.068 \pm 0.005‰$ and $-0.027 \pm 0.006‰$, respectively. Dhajala-1, $\delta^{34}S$ shows a much larger range of variation, from $-1.067‰$ to $0.995‰$ whereas Dhajala-2 exhibits a relatively smaller range with lowest and highest $\delta^{34}S$ of $-0.146‰$ and $0.352‰$, respectively (Table 2). The weighted averages of $\Delta^{33}S$ in Dhajala-1 and Dhajala-2 are $0.025‰$ and $0.016‰$ and are similar, within the experimental uncertainty, whereas they display a relatively larger range of variations ($-0.001‰$–$0.113‰$ for Dhajala-1 and $-0.004‰$–$0.088‰$ for Dhajala-2). $\Delta^{33}S$ of individual steps are presented in Table A1 and plotted in Fig. 5a against cumulative sulfur release. It is apparent that despite possessing normal bulk average values, both chondrule fractions have significant, resolvable ^{33}S excesses in the later stages of sulfur release.

EET99404. Sulfur in chondrules separated from this meteorite were extracted in three steps and have a total of 1.2 wt% sulfur with an average $\delta^{34}S$ value of $0.089 \pm 0.012‰$. $\delta^{34}S$ values range from $-0.155‰$ in the first step, to $1.301‰$ in the second. $\Delta^{33}S$ values, on the other hand, range from $0.001‰$ in the first step, with highest values of $0.032‰$ observed in the last step (Fig. 5c). The average $\Delta^{33}S$ and $\Delta^{36}S$ are $0.003‰$ and $0.189‰$, respectively, which are essentially inseparable from zero to within experimental uncertainty. $\Delta^{33}S$ of individual steps are plotted against cumulative sulfur release in Fig. 5c, and a small excess ^{33}S can be seen in the final step. (Fig. 6).

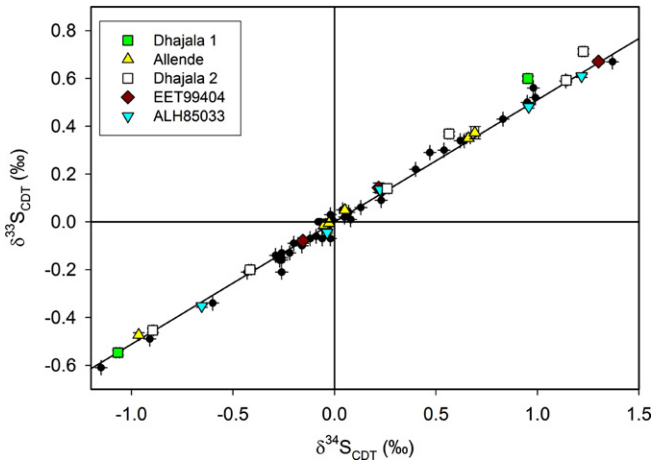

Fig. 6. Plot of $\delta^{33}S$ vs $\delta^{34}S$ for various steps of sulfur extraction from chondrules. Bulk samples from literature are included as black circles for reference. It can be seen that most of the data from the literature lie on the mass fractionation line whereas data points for Dhajala chondrules clearly lie above this line.

Allende. The sulfur isotopic composition of various phases of Allende (CV3) was studied extensively by Gao and Thiemens (1993a). They also studied the sulfur composition in size sorted chondrule fractions. In this study a different approach was pursued, and separation of various sulfur components was achieved based on chemical reactivity. Sulfur was extracted in six steps which contain total 0.9 wt% of sulfur as sulfide phases with a weighted mean

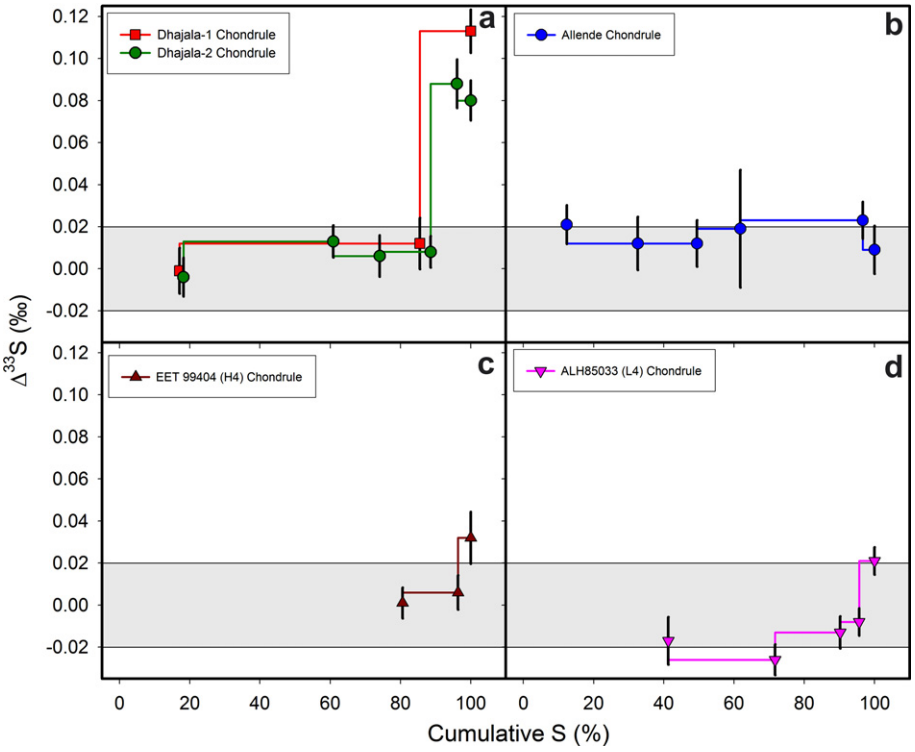

Fig. 5. $\Delta^{33}S$ of various steps are plotted against cumulative sulfur release for physically separated chondrules. The shaded rectangle represents the 2σ error envelope. $\Delta^{33}S$ values are calculated using 0.512 as the exponent.

of $\delta^{34}S = 0.056 \pm 0.007‰$ (Table 2). The $\delta^{34}S$ values range from $-0.965‰$ to $0.660‰$, which is larger than observed earlier for size sorted chondrule fractions ($-0.07‰$–$0.32‰$). $\Delta^{33}S$ values range from $0.009‰$ (last step) to $0.023‰$ (5th step) with a weighted mean of $0.018 \pm 0.013‰$, similar to that observed by Gao and Thiemens (1993a) for bulk chondrule measurements. In Fig. 5b, $\Delta^{33}S$ is plotted against cumulative release of sulfur. It can be seen clearly that sulfur in all the steps falling in or close to the normal envelope defined by a 2σ rectangle except for the fourth extraction step. The weighted average $\Delta^{36}S$ is $-0.039‰$, which is close to normal ($0‰$) within the experimental uncertainty with minimum and maximum values for the steps being $-0.251‰$ (3rd step) and $0.190‰$ (last step), respectively.

ALH85033. Sulfur was extracted in five steps from a chondrule of ALH85033. It contains 0.9 wt% of sulfur as sulfide, with average $\delta^{34}S = 0.006 \pm 0.005‰$ and values ranging from $-0.654‰$ (1st step) and $1.218‰$ (3rd step). $\Delta^{33}S$ values range from $-0.026‰$ to $0.021‰$ with an average for all the steps equal to $-0.017‰$ (Fig. 5d). Although the $\Delta^{33}S$ values are close to or fall within the error envelope, the total internal variation in $\Delta^{33}S$ is $0.047‰$ and is higher than the experimental uncertainty.

4. Discussion

4.1. Kinetic fractionation and nonzero $\Delta^{33}S$

The isotopic fractionation factors are slightly different for equilibrium and kinetic fractionation processes, therefore it is theoretically possible to produce a small $\Delta^{33}S$ values with a series of equilibrium and kinetic fractionation processes (Ono et al., 2006). In the case of chondrite sulfur there are two possibilities where such scenarios are plausibly likely: (1) during meteorite formation processes e.g., condensation and evaporation of sulfur minerals in the solar nebula or parent body processes and (2) during stepwise extraction in the laboratory. The first is unlikely as the chondrites in general, possess a very restricted range for $\delta^{34}S$, not allowing for the needed leverage in isotopic fractionation values. Since the fractionation in the stepwise extraction is kinetic and differs from equilibrium, it is possible that the observed $\Delta^{33}S$ could be an experimental artifact. We assume that a Rayleigh fractionation process occurs in the stepwise extraction process. If ${}^{x}R_{V0}$ is the initial isotope ratio of the sulfur reservoir and which subsequently evolves to ${}^{x}R_{V}$ with a fraction f unreacted then:

$$\frac{{}^{x}R_{V}}{{}^{x}R_{V0}} = f^{{}^{x}\alpha-1}. \tag{9}$$

Where ${}^{x}\alpha$ is the relevant fractionation factor for the process and x is the mass number of isotopes; 33, 34, and 36 in the case of sulfur. All the isotopic ratios are normalized with respect to ^{32}S.

Dividing both numerator and denominator by ${}^{x}R_{\text{std}}$ and replacing the isotope ratios with δ values we obtain:

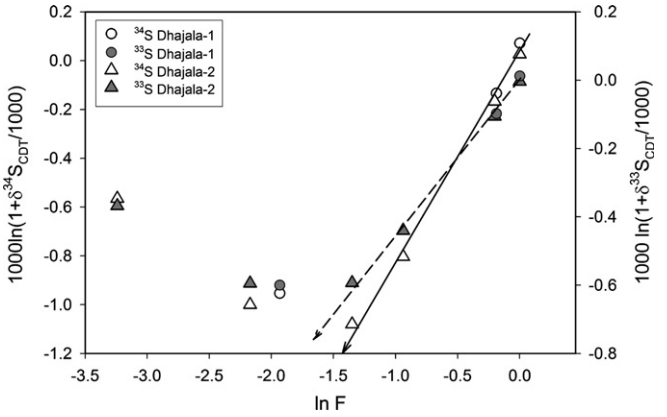

Fig. 7. Plot of $\ln(1+\delta^{34}S/1000)$ and $\ln(1+\delta^{33}S/1000)$ against $\ln f$. If Rayleigh fractionation is responsible for the observed fractionation, all points should fall along the straight line as indicated by the arrow. Deviation of data points away from the line clearly indicates that fractionation mechanism other than kinetic are also operating. (in order to avoid too many zeros y axes are multiplied by 1000).

$$\frac{\left(\frac{\delta^{x}S_{V}}{1000}+1\right)}{\left(\frac{\delta^{x}S_{V0}}{1000}+1\right)} = f^{{}^{x}\alpha-1}.$$

After taking the logarithm:

$$\ln\left(\frac{\delta^{x}S_{V}}{1000}+1\right) = ({}^{x}\alpha-1)\ln f - \ln\left(\frac{\delta^{x}S_{V0}}{1000}+1\right). \tag{10}$$

If $\ln(\frac{\delta^{x}S_{V}}{1000}+1)$ is plotted versus $\ln f$, it should define a straight line with the slope value of $({}^{x}\alpha\text{-}1)$. In Fig. 7 $\ln(\frac{\delta^{33}S_{V}}{1000}+1)$ and $\ln(\frac{\delta^{34}S_{V}}{1000}+1)$ are plotted against $\ln f$ for Dhajala chondrules, it can be seen clearly that the Rayleigh fractionation was operating (as indicated by arrow) during initial steps but in the later steps which have nonzero $\Delta^{33}S$ (last step for Dhajala-1 chondrule and last two steps of Dhajala-2 chondrules) are quite off the line indicating that the nonzero $\Delta^{33}S$ are real and come from the differential reaction rates of different sulfide minerals rather than being an artifact of Rayleigh fractionation.

4.2. Origin of excess ^{33}S

The observation of mass independent sulfur in chondrules (as well as in achondrites; Rai et al., 2005) that formed in distinct nebular regions requires either a wide spread reservoir of mass independent sulfur in the early solar nebula or a region where MIF sulfur is produced and subsequently transported to the meteorite forming region. Mass independent sulfur, like any other isotopic anomaly can be produced by a variety of processes, such as (i) stellar nucleosynthesis, (ii) cosmic ray spallation, (iii) mass independent chemical reactions either in the solar nebula or on the meteorite parent body.

Spallation is ruled out as it produces a nearly constant ratio of $^{36}S/^{33}S \sim 6$ (or $\Delta^{36}S/\Delta^{33}S \sim 8$) in the metallic phase of iron meteorites (Gao and Thiemens, 1991). Unlike, iron

meteorites, which have both higher concentrations of the target element (high Fe/S ratio) as well as the requisite high cosmic ray exposure ages, the analyzed meteorites have insufficient iron concentrations and cosmic ray exposure ages. Spallation with other elements with higher atomic number is less likely because they are relatively less abundant than sulfur in chondrites. Another possibility is that ^{33}S enrichment is produced by thermal neutron capture on ^{32}S on the parent body (if parent body is large enough) but this would enrich ^{33}S homogeneously in all the sulfur phases in chondrites and, the observation of a relatively larger amount of mass dependent sulfur during the initial extraction steps rules out this possibility.

Sulfur isotopes are synthesized in different stellar environments: ^{32}S and ^{34}S are made from hydrostatic and explosive oxygen burning while ^{33}S is produced is made from explosive oxygen and neon burning (Chin et al., 1996; Woosley et al., 2002; Mauersberger et al., 2004). ^{36}S, on the other hand, is produced in very different stellar environments, such as convective shell C-burning in hydrostatic conditions in massive stars prior to the SN II explosion (Woosley and Weaver, 1995). ^{36}S is also the least abundant sulfur isotope and any inhomogeneity due to incomplete mixing of different nucleosynthetic components of sulfur is more apparent in $\delta^{36}S$ variations. Within the analytical uncertainty, the $^{36}S/^{32}S$ of all the steps with excess ^{33}S is constant (Table A1) indicating that the various sulfur nucleosynthetic components in the solar nebula were well homogenized and therefore this possibility can also be ruled out.

The other alternative is that the mass independent sulfur in meteorites is of chemical origin. There are three different ways by which MIF of sulfur can be produced either: (i) hyperfine nuclear spin isotope effects, or (ii) nuclear field shift effect, or (i) gas phase photochemistry in the solar nebula. It has been shown that in the course of chemical reactions involving radical pairs (RP), reaction rates depend on orientation of nuclear spins in the pairs, a manifestation of the exclusion principle. Singlet-triplet and triplet-singlet intersystem crossing (ISCs) in the RP under certain conditions may be induced by hyperfine electron–nuclear interactions which cause simultaneous exchanges in nuclear and electron spin. For example, a triple state may re-phase to become a singlet, which allows for the reaction to occur, which is otherwise forbidden as a triple. In this case the rate of conversion of the triple state to singlet depends upon the magnet interaction between the nucleus and electron. This in turn requires that the nucleus must be magnetic and possess a nuclear spin, otherwise there is no magnetic moment. As such, the reaction rate is dominated by the presence of a nuclear spin. For this reason, the magnetic nuclide dominates in reaction over the non magnetic. This effect is maximized when the radicals pairs are confined to a physical space that serves as a cage that restricts diffusional and rotational motion of the partner of the pair but that also permits reencounters of the partners within a period that allows the nuclear spin to manifest itself in the reaction rate (Turro, 1983). If one radical of the pair diffuses prior to recombination, the identity is lost and the isotopic selection vanishes. For this reason the effect does not occur in the gas phase where diffusion is too rapid. Mass Independent enrichment of ^{33}S of more than 2% has been observed in the photolysis of Phenyl-acyl-phenyl-sulphone in SDS micelles (Step et al., 1990) and is suggested to arise from the magnetic properties of ^{33}S. In this case, there is a very effective solvent medium that restrains the radical pairs in the 'solvent cage' which produces the isotope effect. The other important criterion for formation of a triplet radical is the interaction with an energetic photon. Such a scenario is unlikely under solar nebula conditions though ostensibly possible on a parent body as aqueous alterations occur on many chondritic parent bodies. A solvent, with a high density of organics would be mandatory and there is little evidence, if any, from meteorites that a high molarity organic solution was present.

The nuclear field shift isotope effect is a displacement of ground electronic energy of an atom or molecule due to differences in the nuclear size and shape of an isotope. The magnitude of the shift depends on two factors: (1) electron density at the nucleus and (2) the charge, size and shape of nucleus, and change of the latter two between isotopes (Bigeleisen, 1996). Since the isotopes of an element have the same nuclear charge (number of protons) but different average radius, the field shift is proportional to the isotopic difference in nuclear charge radius (King, 1984). Recently it has been utilized to explain isotopic anomalies found in refractory inclusions of chondrites (Fujii et al., 2006). It has been shown that the field shift effect is intimately related to mass dependent fractionation (or vibrational isotope effect) (Bigeleisen, 1996; Fujii et al., 2006) therefore for visible MIF of ^{33}S, a relatively large mass fractionation is required. For heavy elements like Uranium, mass dependent fractionations are small compared to field shifts (Bigeleisen, 1996) but for sulfur, vibrational effects should be much higher. Therefore any MIF of sulfur due to field shift is also accompanied by a larger change in $\delta^{34}S$ and $\delta^{36}S$. The relatively narrow range of $\delta^{34}S$ in steps with positive $\Delta^{33}S$ rules out such a possibility at present for sulfur.

It has been well established that a mass independent isotopic composition for sulfur and oxygen isotopes can be generated in the Earth's and Martian atmosphere (Farquhar and Thiemens, 2000; Farquhar et al., 2000a, 2002) which may be subsequently transferred to the surface rocks. Mass independent sulfur has also been observed sulfonic acid extracts from the Murchison meteorite (Cooper et al., 1997). In the laboratory, mass independent fractionation of sulfur isotope has been observed in the photopolymerization of CS, CS_2 (Colman et al., 1996) and photolysis of SO_2 and H_2S (Farquhar et al., 2000c, 2001). Photolysis of SO_2 has been studied extensively (Farquhar et al., 2001) and it has been demonstrated that mass independent isotopic fractionation effects are wavelength sensitive. A moderate wavelength dependency has also

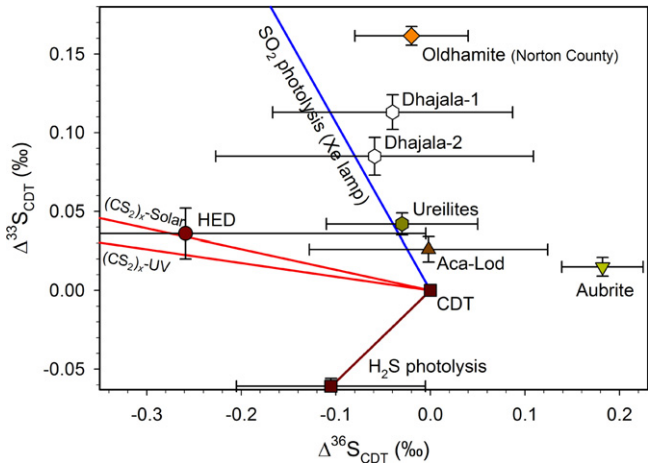

Fig. 8. The $\Delta^{33}S$ vs $\Delta^{36}S$ for various meteorite classes are plotted. Also plotted are mixing line connecting mass independent fractionation observed in laboratory photolysis experiments and mass dependent sulfur [(0,0) on this plot]. Photolysis data are from Farquhar et al. (2000c, 2001) and Colman et al., 1996. Data for meteorites are from Farquhar et al. (2000b) and Rai et al., 2005.

been observed for photopolymerization of CS and CS_2 (Colman et al., 1996). In Fig. 8, mass independent fractionation characteristics for various laboratory experiments are shown. It can be seen that none of the reactions produce only ^{33}S excess without equal or larger effects in ^{36}S, which is not been observed in meteorites. Though the meteoritic data are closer to the SO_2 photolysis line, it is probably irrelevant due to the presumed lack of SO_2 in the early solar nebula. In the H_2S photolysis product, ^{33}S depletion has been observed whereas $\Delta^{36}S$ is zero within experimental uncertainly. It is thus possible that the residual H_2S may be responsible for the observed anomaly. For H_2S, photolysis experiments have been performed for only one wavelength (Farquhar et al., 2000c) and it is possible that like SO_2, fractionation during photolysis is wavelength dependent. Photochemical fractionation data for all these species are needed at shorter wavelengths that are more relevant to early solar nebula (Canuto et al., 1983). Thermodynamic chemical equilibrium models predict that in a nebular gas that is more reduced than solar ($C/O \geqslant 0.95$) but possessing an otherwise solar composition and at higher temperatures, SiS is the most abundant sulfur bearing gas and MgS and CaS compete with FeS as the main sulfide reservoir (Pasek et al., 2005). Thus gas phase SiS may be one of the important species where photochemical fractionation data are required and which may be more relevant for the observed anomaly.

4.3. Carrier of excess ^{33}S

Out of the four chondrule samples studied here, two samples of Dhajala showed clear ^{33}S excesses in the last or last two steps of Dhajala-1 and Dhajala-2, respectively (Fig. 5a). Although these trends in $\Delta^{33}S$ can also be observed in chondrules from EET99404 and ALH85033 in the later steps of sulfur release, the majority of sulfur released in initial steps of ALH85033 is relatively depleted in ^{33}S. Similar to chondrules, Dhajala-1 bulk and Dhajala-2 matrix samples show excess ^{33}S in the final extraction steps but the magnitudes of ^{33}S excesses are relatively smaller. The matrix does not seem to carry excess ^{33}S as inferred from the fairly constant $\Delta^{33}S$ values in all the steps of EET99404 matrix (Fig. 4). Chondrules seem to be a carrier of mass independent sulfur in chondrites. The relatively larger ^{33}S excess in bulk sample of Dhajala as compared to the matrix is most likely coming from chondrules which contribute a large fraction of total mass in chondrites. A small excess in ^{33}S observed in matrices of Dhajala and ALH85033 may be due to fine chondrule fragments in matrix (Scott et al., 1988). In chondrules, most of the sulfur is concentrated mainly in chondrule rims (Hewins, 1997) though a very small fraction (~0.002 wt%) of the total sulfide is carried by chondrule interiors of Dhajala which also has excess ^{33}S (Table A1). This is the only chondrule sample where sulfur measurements were possible after crushing of the pre acid extracted chondrules. During pre extraction nearly all the sulfur in the rims is expected to be removed and further acid extraction after crushing allows sulfur from the chondrule interiors to react with acid. From this single data point, it seems likely that sulfur within the chondrule also has excess ^{33}S, though further investigation is needed to substantiate this. It can be seen that in most cases the highest ^{33}S excess was observed in the later steps of extraction implying that the carrier is relatively slow to react with acid.

In achondrites, we have argued that MIF sulfur was carried by oldhamite (CaS) or refractory sulfide phases (e.g., MgS, Nininggerite; MnS, Alabandite etc.) formed under reducing conditions (Larimer and Bartholomay, 1979) in the solar nebula (Rai et al., 2005). The MIF sulfur was produced by photochemical reactions by solar UV radiation from a UV active protoSun. Most sulfur present in chondrules and their rims has been shown to be carried as troilite, (Lauretta et al., 1996; Tachibana and Huss, 2005), but the presence of refractory sulfides condensed in a reduced nebular gas has been indirectly inferred by peculiar REE patterns observed in two chondrules from ordinary chondrites (Pack et al., 2004). It is also possible that initially MIF sulfur was preserved as refractory sulfide phases, which is unstable under oxidizing conditions in the solar nebula or inside a chondrite parent body and subsequently transformed to troilite. Mass independent sulfur reservoirs could be produced by UV photolysis reactions by high energy UV irradiation from the protoSun as suggested by Rai et al. (2005).

4.4. Sulfur isotopic constraint for the formation of chondrules and their rims

There are many models proposed for the origin of chondrules and their rims (Boss, 1996; Hewins, 1997). All of these aim to explain following properties of chondrules:

Table A1
Sulfur isotope composition of various physically separated components of chondrites

Sample name	Conc.	With respect to CDT							
	% wt. S	$\delta^{33}S$	±Error	$\delta^{34}S$	±Error	$\delta^{36}S$	±Error	$\Delta^{33}S$	$\Delta^{36}S$
Allende (CV3) chondrule									
T1	0.11	−0.473	0.009[a]	−0.965	0.004	−1.797	0.136	0.021	0.031
T2	0.18	−0.014	0.012	−0.051	0.008	−0.124	0.151	0.012	−0.027
T3	0.15	0.350	0.010	0.660	0.009	1.010	0.110	0.012	−0.251
T4	0.11	0.373	0.026	0.692	0.019	1.462	0.428	0.019	0.149
T5	0.31	0.049	0.008	0.051	0.007	0.040	0.113	0.023	−0.057
T6 + heat	0.03	−0.005	0.011	−0.027	0.006	0.138	0.120	0.009	0.190
Weighted mean[b]	0.89	0.061	0.012	0.084	0.009	0.122	0.162	0.018	−0.039
Allende (CV3) broken chondrule									
BT1	0.046	−0.745	0.010	−1.434	0.005	−2.886	0.126	−0.011	−0.170
BT2	0.155	−0.771	0.010	−1.527	0.004	−3.145	0.083	0.010	−0.230
BT3	0.101	0.301	0.010	0.616	0.008	0.871	0.101	0.014	−0.297
BT4	0.084	−0.286	0.008	−0.584	0.004	−1.120	0.086	0.013	−0.014
BT5	0.044	−0.238	0.009	−0.506	0.004	−1.190	0.082	0.021	−0.231
BT6	0.714	0.178	0.008	0.323	0.004	0.481	0.113	0.013	−0.132
BT7	0.079								
BT8	0.370								
BT9	0.104	0.223	0.013	0.384	0.004	0.562	0.126	0.027	−0.172
BT10 + heat	0.080	0.130	0.006	0.203	0.007	0.246	0.110	0.026	−0.142
Mean	1.777								
Dhajala-1 (H3.8) bulk									
T1	0.63	−0.477	0.010	−0.937	0.008	−1.585	0.165	0.002	0.190
T2	0.53	−0.180	0.009	−0.377	0.003	−0.685	0.060	0.013	0.035
T3	0.78	0.467	0.008	0.869	0.006	1.838	0.068	0.023	0.178
T4 + heat	0.035	0.115	0.016	0.087	0.008	0.064	0.177	0.071	−0.102
Weighted mean	1.98	−0.014	0.009	−0.055	0.006	0.038	0.099	0.014	0.138
Dhajala-1 (H3.8) chondrule									
T1	0.13	−0.547	0.010	−1.067	0.008	−2.009	0.084	−0.001	0.012
T2	0.52	−0.008	0.012	−0.039	0.004	−0.259	0.110	0.012	−0.185
T3 + heat	0.11	0.600	0.010	0.953	0.005	1.781	0.126	0.113	−0.040
Crushed	0.002	0.636	0.013	0.995	0.007	1.973	0.128	0.127	0.072
Mean	0.76	−0.011	0.011	−0.068	0.005	−0.257	0.108	0.025	−0.129
Dhajala-1 (H3.8) chondrule + matrix									
CM-T1	1.12	−0.159	0.013	−0.308	0.008	−0.625	0.169	−0.001	−0.041
CM-T2 + heat	0.58	0.469	0.009	0.855	0.004	1.691	0.082	0.032	0.057
Weighted mean	1.70	0.055	0.012	0.089	0.007	0.165	0.139	0.010	−0.008
Dhajala-1 (H3.8) sulfate									
SO_4^-	0.004	1.404	0.019	2.441	0.011	2.527	0.435	0.148	−2.140
Dhajala-2 (H3.8) matrix									
T1	0.78	−0.071	0.005	−0.146	0.003	−0.108	0.102	0.004	0.169
T2	1.34	0.188	0.004	0.352	0.003	0.720	0.070	0.008	0.048
T3 + heat	0.17	0.188	0.008	0.287	0.008	0.726	0.159	0.041	0.178
Weighted mean	2.29	0.100	0.005	0.178	0.003	0.438	0.088	0.009	0.098
Dhajala-2 (H3.8) chondrule									
T1	0.163	−0.454	0.009	−0.895	0.004	−1.745	0.144	−0.004	−0.049
T2	0.382	−0.200	0.007	−0.416	0.006	−1.003	0.116	0.013	−0.214
T3	0.118	0.139	0.009	0.260	0.008	0.362	0.067	0.006	−0.130
T4	0.13	0.592	0.007	1.142	0.005	1.950	0.142	0.008	−0.215
T5	0.067	0.713	0.011	1.226	0.007	2.249	0.136	0.088	−0.075
T6	0.035	0.368	0.009	0.565	0.006	1.044	0.229	0.080	−0.028
Weighted mean	0.895	0.004	0.008	−0.027	0.006	−0.206	0.124	0.016	−0.155
EET99404 (H4) matrix									
T1	0.943	−0.100	0.008	−0.215	0.004	−0.533	0.132	0.010	−0.126
T2	0.052	0.195	0.009	0.377	0.012	0.632	0.124	0.002	−0.088
T3	0.124	−0.016	0.007	−0.039	0.008	−0.041	0.139	0.004	0.033
T4 + heat	0.276	0.008	0.005	0.010	0.005	−0.041	0.099	0.003	−0.060
Weighted mean	1.395	−0.060	0.007	−0.133	0.005	−0.349	0.126	0.008	−0.097

(*continued on next page*)

Table A1 (*continued*)

Sample name	Conc.	With respect to CDT							
	% wt. S	$\delta^{33}S$	±Error	$\delta^{34}S$	±Error	$\delta^{36}S$	±Error	$\Delta^{33}S$	$\Delta^{36}S$
EET99404 (H4) chondrule									
T1	0.998	−0.078	0.004	−0.155	0.012	−0.013	0.110	0.001	0.281
T2	0.196	0.671	0.007	1.301	0.008	2.271	0.119	0.006	−0.215
T3 + heat	0.044	0.143	0.007	0.217	0.020	0.324	0.299	0.032	−0.091
Weighted mean	1.238	0.048	0.005	0.089	0.012	0.361	0.118	0.003	0.189
ALH85033 (L4) matrix									
T1	1.39	−0.100	0.009	−0.214	0.005	−0.533	0.132	0.010	−0.126
T2 + heat	0.45	0.545	0.007	1.007	0.007	1.821	0.119	0.031	−0.088
Weighted mean	1.84	0.058	0.009	0.085	0.005	0.043	0.129	0.015	−0.117
ALH85033 (L4) chondrule									
T1	0.38	−0.352	0.011	−0.654	0.005	−1.283	0.095	−0.017	−0.044
T2	0.28	−0.044	−0.007	−0.036	0.004	−0.074	0.092	−0.026	−0.005
T3	0.17	0.610	0.007	1.218	0.006	2.228	0.110	−0.013	−0.100
T4	0.05	0.481	0.006	0.957	0.005	1.753	0.111	−0.008	−0.076
T5 + heat	0.04	0.136	0.006	0.224	0.005	0.288	0.111	0.021	−0.140
Weighted mean	0.92	−0.014	0.004	0.006	0.005	−0.033	0.098	−0.017	−0.048
Hvittis (EL6) bulk									
T1	1.20	−0.389	0.007	−0.699	0.005	−1.104	0.065	−0.031	0.220
T2	0.591	−0.117	0.011	−0.156	0.006	−0.412	0.090	−0.037	−0.114
T3	0.634	0.417	0.008	0.877	0.005	1.570	0.071	−0.031	−0.106
T4	0.361	0.042	0.009	0.125	0.006	0.173	0.124	−0.022	−0.066
T5	0.130	1.146	0.008	2.265	0.004	4.369	0.077	−0.012	0.038
T6 + heat	0.063	−0.737	0.006	−1.467	0.005	−2.835	0.097	0.014	−0.035
Weighted mean	2.979	−0.052	0.008	−0.043	0.005	−0.041	0.080	−0.029	0.037
Com Ag_2S-oxidized (normalize with respect of single shot extraction of same Ag2S#3)									
T1 (Ag2S#1)	2.11	−7.577	0.011	−14.79	0.01	−27.99	0.151	0.014	0.060
T2 (Ag2S#1)	8.35	1.213	0.015	2.317	0.006	4.497	0.122	0.000	−0.037
T3 (Ag2S#1)	1.82	3.776	0.011	7.353	0.008	14.08	0.106	0.021	−0.011
Weighted mean	12.28	0.083	0.014	0.124	0.007	0.335	0.125	0.006	−0.016
Ag_2S#1 (Ag_2S#2)		0.048	0.011	0.134	0.008	0.372	0.154	−0.020	0.119
Ag2S#2		0.027	0.007	0.046	0.005	0.362	0.095	0.004	0.275
Ag2S#3		0	0.015	0	0.005	0	0.125	0	0
Ag2S#3 (CDT)		0.665	0.015	1.214	0.005	1.816	0.125	0.040	−0.504

Sulfur is extracted by sequential leaching to resolve components of various chemical resistance. All the data was reduced using 0.512 and 1.895 for calculation of $\Delta^{33}S$ and $\Delta^{36}S$, respectively, which is obtained by fractionation experiments done in our laboratory.

[a] Error reported for individual samples are the root mean square error of three repeated measurements (in most cases).

[b] Abundance weighted mean is obtained by summation of abundance multiplied by value (either δ or error) divided by total abundance. In the weighted mean calculation, weighing error has not been propagated.

(i) flash heating that can heat chondrule precursors temperature higher than 1600K, followed by rapid cooling which requires environment that facilitate fast cooling of chondrules, (ii) rims are quite common in chondrules and the mechanism which produce chondrules also participates in rim formation, (iii) it should explain size sorting of chondrules among chondrites and (iv) since chondrules are present in all chondrite classes which formed and accreted in very different physicochemical environment in the solar nebula, any chondrule forming process should be wide spread in the nebula or if it is formed in localized region, requires an appropriate transportation mechanism through which chondrules transported from this location to the region where chondrites were accreting. Observation of mass independent sulfur of photochemical origin places an additional constraint on these models. Chondrules that formed in the nebular disk that requires it to be optically thin such that sulfur rich precursor gas could irradiated by UV light from the protoSun (Rai et al., 2005). Though x-wind and nebular shock wave models (Connolly and Love, 1998; Ciesla and Hood, 2002) can explain several of these properties if not all, production of MIF sulfur via the x-wind model is favorable because it is only this model that affords a mechanism for chondrule precursors to be irradiated with high energy UV light from the early Sun (Shu et al., 1996, 1997). In the x-wind model, mass independent sulfur produced either in the x-region or along the edges of the disk that could see direct UV light from sun as material move towards the x-region with time, as suggested by Rai et al. (2005). Upon reaching the x-region, MIF sulfur is incorporated into chondrules, or condensed as a rim during its traversal back to the disk by an x-wind. In a nebular shock model, chondrules are formed near the mid plane of the optically opaque accretion disk with a highly enhanced

dust/gas ratio (Hood and Horanyi, 1993; Ciesla and Hood, 2002), and hence it is difficult to explain the presence of MIF sulfur within the framework of the present model.

5. Conclusions

Here, we have shown the presence of mass independent sulfur in chondritic meteorites. This sulfur is mostly carried by chondrule rims but phases in the chondrule interior can not be ruled out at present. The new stepwise extraction technique developed here exerts an important role in resolving mass independent sulfur which would, otherwise not have been possible to recognize due to mixing with large amounts of normal sulfur. The observation of mass independent sulfur of photochemical origin in several differentiated and undifferentiated meteorites identifies the importance of photochemistry in the early solar nebula. None of the photolysis experiments involving various gaseous species of sulfur can produce only ^{33}S excess and further experiments more importantly at the shorter wave lengths relevant to the early solar nebula are required. Among the various models for chondrules formation, the x-wind model is more favorable as it is capable of irradiating precursor material with direct UV light from the protoSun.

Acknowledgments

NASA Cosmochemistry program is gratefully acknowledged for the support of this study. We thank Antarctic Meteorite Working Group, Field Museum of Natural History, Chicago and J.N. Goswami for providing meteorite samples for this study. Discussion with Subrata Chakraborty was very helpful in shaping up this manuscript. V.K.R. thanks Terri Jackson and Gerardo Dominguez for their help. Boswell Wing, Dante S. Lauretta and an anonymous reviewer are thanked for helpful reviews.

Associate editor: James Farquhar

Appendix A

See Table A1.

References

Bigeleisen, J., 1996. Nuclear size and shape effects in chemical reactions. Isotope chemistry of the heavy elements. *J. Am. Chem. Soc.* **118**, 3676–3680.

Bigeleisen, J., Mayer, M., 1947. Calculation of equilibrium constants for isotopic exchange reactions. *J. Chem. Phys.*, 15261–15267.

Boss, A.P., 1996. A coincise guide to chondrule fromation models. In: Hewins, R.H., Jones, R.H., Scott, E.R.D. (Eds.), *Chondrules and Protoplanetary Disk*. Cambridge University Press, Cambridge, UK, pp. 257–263.

Canuto, V.M., Levine, J.S., Augustsson, T.R., Imhoff, C.L., Giampapa, M.S., 1983. The young Sun and the atmosphere and photochemistry of the early Earth. *Nature* **305**, 281–286.

Chin, Y.N., Henkel, C., Whiteoak, J.B., Langer, N., Churchwell, E.B., 1996. Interstellar sulfur isotopes and stellar oxygen burning. *Astron. Astrophys.* **305**, 960–969.

Ciesla, F.J., Hood, L.L., 2002. The nebular shock wave model for chondrule formation: Shock processing in a particle-gas suspension. *Icarus* **158**, 281–293.

Colman, J.J., Xu, X.P., Thiemens, M.H., Trogler, W.C., 1996. Photopolymerization and mass-independent sulfur isotope fractionations in carbon disulfide. *Science* **273**, 774–776.

Connolly, H.C., Love, S.G., 1998. The formation of chondrules: petrologic tests of the shock wave model. *Science* **280**, 62–67.

Cooper, G.W., Thiemens, M.H., Jackson, T.L., Chang, S., 1997. Sulfur and hydrogen isotope anomalies in meteorite sulfonic acids. *Science* **277**, 1072–1074.

Desch, S.J., Connolly, H.C., 2002. A model of the thermal processing of particles in solar nebula shocks: application to the cooling rates of chondrules. *Meteorit. Planet. Sci.* **37**, 183–207.

Farquhar, J., Thiemens, M.H., 2000. Oxygen cycle of the Martian atmosphere-regolith system: Delta O-17 of secondary phases in Nakhla and Lafayette. *J. Geophys. Res.* **105**, 11991–11997.

Farquhar, J., Bao, H., Thiemens, M.H., 2000a. Atmospheric influence of Earth's earliest sulfur cycle. *Science* **289**, 756–758.

Farquhar, J., Jackson, T.L., Thiemens, M.H., 2000b. A ^{33}S enrichment in ureilite meteorites: evidence for a nebular sulfur component. *Geochim. Cosmochim. Acta* **64**, 1819–1825.

Farquhar, J., Savarino, J., Jackson, T.L., Thiemens, M.H., 2000c. Evidence of atmospheric sulphur in the martian regolith from sulphur isotopes in meteorites. *Nature* **404**, 50–52.

Farquhar, J., Savarino, J., Airieau, S., Thiemens, M.H., 2001. Observation of wavelength-sensitive mass-independent sulfur isotope effects during SO2 photolysis: Implications for the early atmosphere. *J. Geophys. Res.* **106**, 32829–32839.

Farquhar, J., Wing, B.A., McKeegan, K.D., Harris, J.W., Cartigny, P., Thiemens, M.H., 2002. Mass-independent sulfur of inclusions in diamond and sulfur recycling on early earth. *Science* **298**, 2369–2372.

Forrest, J., Newman, L., 1977. Ag-110 microgram sulfate analysis for short time resolution of ambient levels of sulfur aerosol. *Anal. Chem.* **49**, 1579–1584.

Fujii, T., Moynier, F., Albarede, F., 2006. Nuclear field vs nucleosynthetic effects as cause of isotopic anomalies in the early solar system. *Earth Planet. Sci. Lett.* **247**, 1–9.

Gao, Y.Q., Marcus, R.A., 2001. Strange and unconventional isotope effects in ozone formation. *Science* **293**, 259–263.

Gao, X., Thiemens, M.H., 1991. Systematic study of sulfur isotopic composition in iron-meteorites and the occurrence of excess ^{33}S and ^{36}S. *Geochim. Cosmochim. Acta* **55**, 2671–2679.

Gao, X., Thiemens, M.H., 1993a. Isotopic composition and concentration of sulfur in carbonaceous chondrites. *Geochim. Cosmochim. Acta* **57**, 3159–3169.

Gao, X., Thiemens, M.H., 1993b. Variations of the isotopic composition of sulfur in enstatite and ordinary chondrites. *Geochim. Cosmochim. Acta* **57**, 3171–3176.

Grossman, J.N., 1988. Meteorites—chondrites and the solar nebula. *Nature* **334**, 14–15.

Hewins, R.H., 1997. Chondrules. *Annu. Rev. Earth Planet. Sci.* **25**, 61–83.

Hood, L.L., Horanyi, M., 1993. The nebular shock-wave model for chondrule formation—one-dimensional calculations. *Icarus* **106**, 179–189.

Hulston, J.R., Thode, H.G., 1965. Variations in the S^{33}, S^{34} and S^{36} contents of meteorites and their relation to chemical and nuclear effects. *J. Geophys. Res.* **70**, 3475–3484.

King, W.H., 1984. *Isotope Shifts in Atomic Spectra*. Plenum Press.

Larimer, J.W., Bartholomay, M., 1979. Role of carbon and oxygen in cosmic gases—some applications to the chemistry and mineralogy of enstatite chondrites. *Geochim. Cosmochim. Acta* **43**, 1455–1466.

Lauretta, D.S., Kremser, D.T., Fegley, B., 1996. The rate of iron sulfide formation in the solar nebula. *Icarus* **122**, 288–315.

Mauersberger, R., Ott, U., Henkel, C., Cernicharo, J., Gallino, R., 2004. The abundance of 36S in IRC + 10216 and its production in the Galaxy. *Astron. Astrophys.* **426**, 219–227.

Miller, M.F., 2002. Isotopic fractionation and the quantification of O-17 anomalies in the oxygen three-isotope system: An appraisal and geochemical significance. *Geochim. Cosmochim. Acta* **66**, 1881–1889.

Miller, M.F., Franchi, I.A., Thiemens, M.H., Jackson, T.L., Brack, A., Kurat, G., Pillinger, C.T., 2002. Mass-independent fractionation of oxygen isotopes during thermal decomposition of carbonates. *Proc. Natl. Acad. Sci. USA* **99**, 10988–10993.

Ono, S., Wing, B., Johnston, D., Farquhar, J., Rumble, D., 2006. Mass-dependent fractionation of quadruple stable sulfur isotope system as a new tracer of sulfur biogeochemical cycles. *Geochim. Cosmochim. Acta* **70**, 2238–2252.

Pack, A., Shelley, J.M.G., Palme, H., 2004. Chondrules with peculiar REE patterns: Implications for solar nebular condensation at high C/O. *Science* **303**, 997–1000.

Pasek, M.A., Milsom, J.A., Ciesla, F.J., Lauretta, D.S., Sharp, C.M., Lunine, J.I., 2005. Sulfur chemistry with time-varying oxygen abundance during solar system formation. *Icarus* **175**, 1–14.

Rai, V.K., Jackson, T.L., Thiemens, M.H., 2005. Photochemical mass-independent sulfur isotopes in achondritic meteorites. *Science* **309**, 1062–1065.

Rees, C.E., Thode, H.G., 1977. S-33 anomaly in allende meteorite. *Geochim. Cosmochim. Acta* **41**, 1679–1682.

Romero, A.B., Thiemens, M.H., 2003. Mass-independent sulfur isotopic compositions in present-day sulfate aerosols. *J. Geophys. Res.*, 108.

Ruzicka, A., Snyder, G.A., Taylor, L.A., 2000. Crystal-bearing lunar spherules: Impact melting of the Moon's crust and implications for the origin of meteoritic chondrules. *Meteorit. Planet. Sci.* **35**, 173–192.

Scott, E.R.D. et al., 1988. Primitive material surviving in chondrites: matrix. In: Kerrdge, J.F., Matthews, M.S. (Eds.), *Meteorites and Early Solar System*. University of Arizona Press, Tucson, pp. 718–745.

Sears, D.W.G., 2004. *The Origin of Chondrules and Chondrites*. Cambridge University Press, Cambridge, UK.

Shu, F.H., Shang, H., Lee, T., 1996. Toward an astrophysical theory of chondrites. *Science* **271**, 1545–1552.

Shu, F.H., Shang, H., Glassgold, A.E., Lee, T., 1997. X-rays and fluctuating x-winds from protostars. *Science* **277**, 1475–1479.

Step, E.N., Tarasov, V.F., Buchachenko, A.L., 1990. Magnetic isotope effect. *Nature* **345**, 25.

Symes, S.J.K., Sears, D.W.G., Akridge, D.G., Huang, S.X., Benoit, P.H., 1998. The crystalline lunar spherules: their formation and implications for the origin of meteoritic chondrules. *Meteorit. Planet. Sci.* **33**, 13–29.

Tachibana, S., Huss, G.R., 2005. Sulfur isotope composition of putative primary troilite in chondrules from Bishunpur and Semarkona. *Geochim. Cosmochim. Acta* **69**, 3075–3097.

Taylor, G.J., Scott, E.R.D., Keil, K., 1983. Cosmic setting for chondrule formation. In: King, E.A. (Ed.), *Chondrules and their Origins*. Lunar Planet. Inst., Houston, pp. 262–278.

Thiemens, M.H., 1999. Atmosphere science—mass-independent isotope effects in planetary atmospheres and the early solar system. *Science* **283**, 341–345.

Thiemens, M.H., 2006. History and applications of mass-independent isotope effects. *Annu. Rev. Earth Planet. Sci.* **34**, 217–262.

Thiemens, M.H., Heidenreich, J.E., 1983. The mass-independent fractionation of oxygen—a novel isotope effect and its possible cosmochemical implications. *Science* **219**, 1073–1075.

Tudge, A.P., Thode, H.G., 1950. Thermodynamic properties of isotopic compounds of sulfur. *Can. J. Res* **28**, 567–578.

Turro, N.J., 1983. Influence of Nuclear-Spin on Chemical-Reactions - Magnetic Isotope and Magnetic-Field Effects (A Review). *Proc. Natl. Acad. Sci. USA* **80**, 609–621.

Urey, H.C., 1947. Thermodynamics of isotopic substances. *J. Chem. Soc.*, 562–581.

Woosley, S.E., Weaver, T.A., 1995. The evolution and explosion of massive stars 2. Explosive hydrodynamics and nucleosynthesis. *Astrophys. J Suppl. S.* **101**, 181–235.

Woosley, S.E., Heger, A., Weaver, T.A., 2002. The evolution and explosion of massive stars. *Rev. Mod. Phys.* **74**, 1015–1071.